© 2015. Published by The Company of Biologists Ltd | Development (2015) 142, 1050-1061 doi:10.1242/dev.119180

RESEARCH ARTICLE

STEM CELLS AND REGENERATION

Gata2b is a restricted early regulator of hemogenic endothelium in the zebrafish embryo

Emerald Butko[1], Martin Distel[1,*], Claire Pouget[1], Bart Weijts[1], Isao Kobayashi[1], Kevin Ng[1], Christian Mosimann[2], Fabienne E. Poulain[3,‡], Adam McPherson[3], Chih-Wen Ni[4,§], David L. Stachura[1,¶], Natasha Del Cid[1], Raquel Espín-Palazón[1], Nathan D. Lawson[4], Richard Dorsky[3], Wilson K. Clements[1,5] and David Traver[1,6,]**

ABSTRACT

The adult blood system is established by hematopoietic stem cells (HSCs), which arise during development from an endothelial-to-hematopoietic transition of cells comprising the floor of the dorsal aorta. Expression of aortic *runx1* has served as an early marker of HSC commitment in the zebrafish embryo, but recent studies have suggested that HSC specification begins during the convergence of posterior lateral plate mesoderm (PLM), well before aorta formation and *runx1* transcription. Further understanding of the earliest stages of HSC specification necessitates an earlier marker of hemogenic endothelium. Studies in mice have suggested that GATA2 might function at early stages within hemogenic endothelium. Two orthologs of *Gata2* exist in zebrafish: *gata2a* and *gata2b*. Here, we report that *gata2b* expression initiates during the convergence of PLM, becoming restricted to emerging HSCs. We observe Notch-dependent *gata2b* expression within the hemogenic subcompartment of the dorsal aorta that is in turn required to initiate *runx1* expression. Our results indicate that Gata2b functions within hemogenic endothelium from an early stage, whereas Gata2a functions more broadly throughout the vascular system.

KEY WORDS: Hematopoietic stem cell, Hemogenic endothelium, Subfunctionalization, Gata2, Notch

INTRODUCTION

Hematopoietic stem cells (HSCs) are tissue-specific stem cells that give rise to, and ultimately maintain, the adult blood system over a lifetime. During embryogenesis, HSCs arise from a population of hemogenic endothelium, primarily within the ventral wall of the dorsal aorta (DA) (Ciau-Uitz et al., 2014; Clements and Traver, 2013; Dzierzak and Speck, 2008; Swiers et al., 2013; Taoudi and Medvinsky, 2007). Aortic endothelium transdifferentiates into HSCs via an endothelial-to-hematopoietic transition (EHT) (Chen et al., 2009; Jaffredo et al., 1998; Zovein et al., 2008), a process that is conserved across vertebrates (Bertrand et al., 2010; Boisset et al., 2014, 2010; Chen et al., 2009; Jaffredo et al., 2000, 1998; Kissa and Herbomel, 2010; Lam et al., 2010). EHT produces hematopoietic stem and progenitor cells (HSPCs) that rapidly enter circulation in zebrafish (Bertrand et al., 2010; Boisset et al., 2010; Kissa and Herbomel, 2010; Lam et al., 2010) or proliferate and differentiate locally to form hematopoietic clusters in the chick and mammalian embryo (Boisset et al., 2014; Jaffredo et al., 2000; North et al., 2002; Tavian et al., 1999; Yokomizo and Dzierzak, 2010). Nascent HSPCs home to the caudal hematopoietic tissue (CHT) of zebrafish and to the placenta and fetal liver in mammals, where they undergo proliferation and maturation. Finally, HSCs colonize the kidney in zebrafish and the bone marrow in mammals, where they establish residence for the remainder of life.

The zebrafish model has proven valuable to our understanding of HSPC development, including the first direct *in vivo* visualization of their emergence (Bertrand et al., 2010; Kissa and Herbomel, 2010; Lam et al., 2010). The transcription factor Runx1 is required for EHT in both mice and zebrafish (Chen et al., 2009; Kissa and Herbomel, 2010; Lancrin et al., 2009). Within the zebrafish embryo, *runx1* marks the subpopulation of cells within the DA with hemogenic potential from as early as 23 h post-fertilization (hpf) (Wilkinson et al., 2009), providing one of the earliest reported markers of HSC commitment. However, there is evidence that hemogenic identity is established earlier than the onset of *runx1* expression. We have recently reported that, during the convergence of the posterior lateral plate mesoderm (PLM) prior to the formation of the DA or its rudiment, the vascular cord, contact between the ventral somite and the PLM is necessary to transmit requisite Notch signals into HSC precursors (Kobayashi et al., 2014). That somite-to-PLM signaling occurs between 14 and 18 hpf indicates that cells acquire hemogenic endothelial identity earlier than previously appreciated. Therefore, determining additional markers that distinguish HSCs from vascular cells is essential to investigate early events in HSC specification. In the present study, we identified a novel early hemogenic endothelial marker, *gata2b*, in zebrafish.

Expression of *Gata2* is driven by activation of the NOTCH1 receptor and its transcriptional partner RBPjκ in the DA of mice (Robert-Moreno et al., 2005). Mice deficient in GATA2 die at embryonic day (E) 10.5 with defects in primitive and definitive hematopoiesis (Tsai et al., 1994). Targeted deletion of *Gata2* within the endothelium results in edema, hemorrhage and loss of functional HSCs (de Pater et al., 2013; Johnson et al., 2012; Lim et al., 2012). In addition, GATA2 serves iterative roles in early vascular cells and their hemogenic progeny (de Pater et al., 2013). GATA2 is required within the endothelium for the expression of *Runx1* (Gao et al., 2013) that is essential for EHT (Chen et al., 2009; Kissa and

[1]Department of Cellular and Molecular Medicine, University of California at San Diego, La Jolla, CA 92093, USA. [2]Institute of Molecular Life Sciences, University of Zürich, Zürich, Switzerland. [3]Department of Neurobiology and Anatomy, University of Utah, Salt Lake City, UT 84132, USA. [4]University of Massachusetts at Worcester, Worcester, MA 01605, USA. [5]Department of Hematology, St Jude Children's Research Hospital, Memphis, TN 38105, USA. [6]Section of Cell and Developmental Biology, Division of Biological Sciences, University of California at San Diego, La Jolla, CA 92093, USA.
*Present address: St Anna Kinderkrebsforschunge e.V., Children's Cancer Research Institute, Vienna, Austria. ‡Present address: Department of Biological Sciences, University of South Carolina, Columbia, SC 29208, USA. §Present address: Department of Biomedical Engineering, Khalifa University, Abu Dhabi, UAE. ¶Present address: Department of Biological Sciences, California State University, Chico, CA 95929, USA.

**Author for correspondence (dtraver@ucsd.edu)

Received 28 October 2014; Accepted 29 January 2015

Development (2015) 142, 1050-1061 doi:10.1242/dev.119180

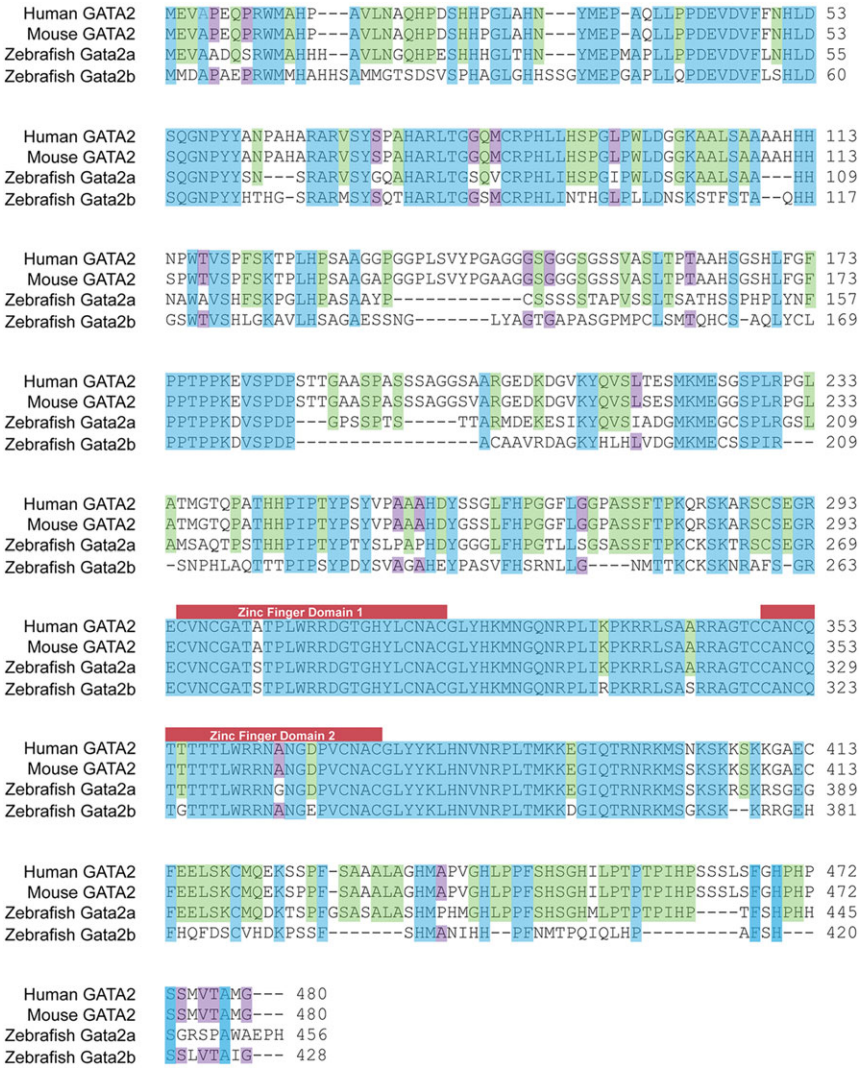

Fig. 1. Homology of Gata2a and Gata2b proteins. Alignment of amino acid sequences of human GATA2, murine GATA2, and zebrafish Gata2a and Gata2b sequences. Residues conserved in all four proteins are highlighted in blue. Residues conserved between human GATA2, murine GATA2 and zebrafish Gata2a are highlighted in green. Residues conserved between human GATA2, murine GATA2 and zebrafish Gata2b are highlighted in purple.

Herbomel, 2010; Lancrin et al., 2009), and this is likely to be through direct regulation of a hemogenic endothelial-specific *Runx1* enhancer (Nottingham et al., 2007). Together, these studies suggest that GATA2 functions downstream of Notch signaling within the endothelium to activate *Runx1* expression.

A genome duplication event in early teleosts generated two *gata2* paralogs in the zebrafish genome (Gillis et al., 2009). The *gata2a* paralog is expressed throughout the PLM and trunk vasculature (Brown et al., 2000; Detrich et al., 1995) but is not affected by the loss of Notch signaling downstream of Wnt16, which affects HSC but not arterial specification (Clements et al., 2011). Additionally, the loss of Gata2a in *gata2a*^{um27} mutants results in defects in vascular morphogenesis and circulation (Zhu et al., 2011), making it difficult to address possible hematopoietic functions of Gata2a. In this study, we focus on the *gata2b* paralog in the context of HSC specification. We show that *gata2b* is expressed specifically within hemogenic endothelium prior to *runx1*. We generated *gata2b:Gal4* transgenic animals, which specifically label hemogenic endothelium and nascent HSCs. Moreover, *gata2b* is required genetically upstream of *runx1*. Whereas *gata2a* is required for vascular development and circulation (Zhu et al., 2011), *gata2b* is not required for these processes. Our findings suggest that the duplication event resulting in *gata2a* and *gata2b* has segregated the endothelial and hematopoietic functions of Gata2 in zebrafish, allowing for future studies of the hemogenic function of Gata2 without disruption of the vasculature or circulation.

RESULTS

gata2b is expressed in hematopoietic precursor cells

A chromosomal duplication event in the teleost lineage resulted in two zebrafish paralogs of Gata2, *gata2a* and *gata2b* (Gillis et al., 2009), which share only 57% sequence identity and 67% similarity (Fig. 1). Although *gata2b* has been identified in the genome, little is known about its expression or function. To better understand *gata2b*, we explored its expression during embryogenesis by quantitative PCR (qPCR) and whole-mount *in situ* hybridization (WISH). *gata2b* is maternally expressed, and embryonic transcription initiated at 16 hpf (Fig. 2A). By WISH, no expression of *gata2b* was observed in the developing early PLM, in contrast to *gata2a*, which is expressed in the PLM from approximately the 3-somite stage, at ∼10.3 hpf (Li et al., 2009) (supplementary material Fig. S1). By 18 hpf, expression of *gata2b* is detectable in a small number of cells at and near the midline

Development (2015) 142, 1050-1061 doi:10.1242/dev.119180

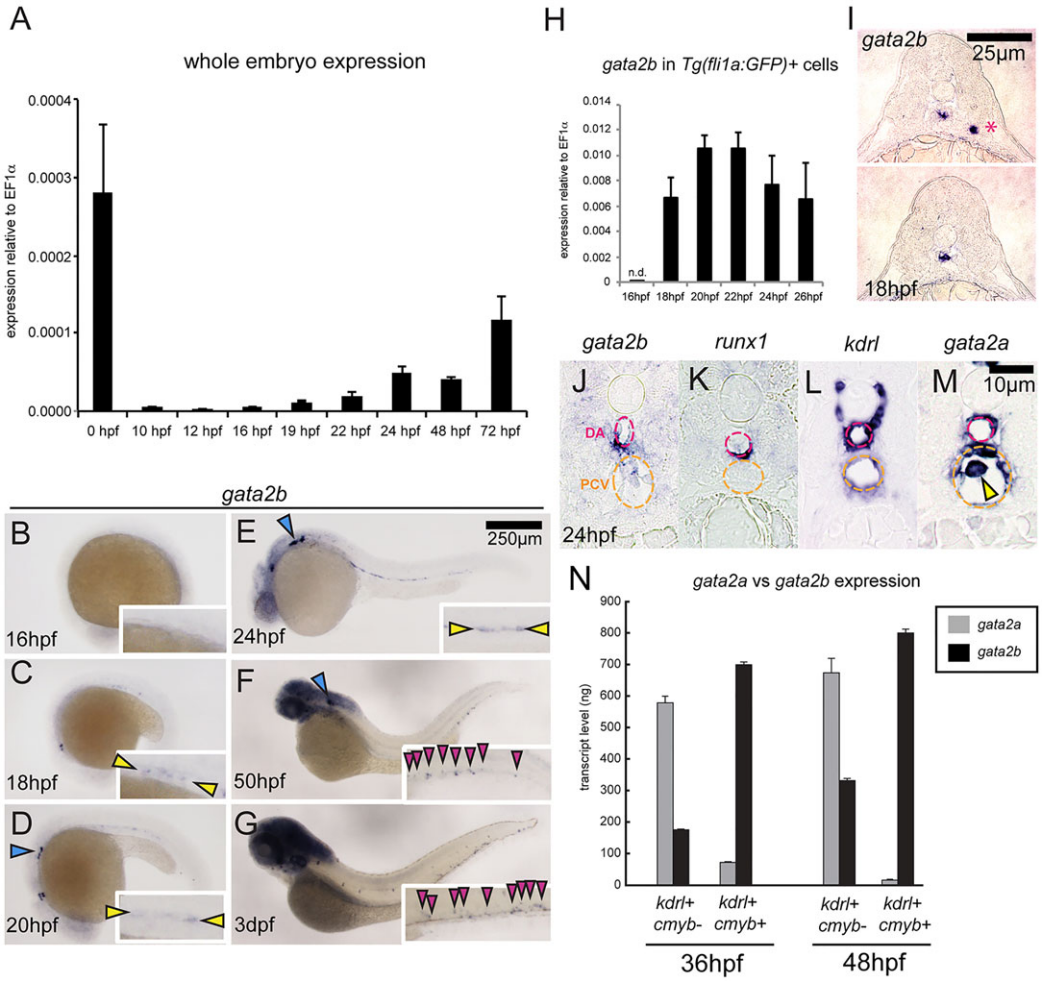

Fig. 2. Zebrafish *gata2b* is expressed in hemogenic endothelium. (A) Expression of *gata2b* in whole embryos over time. cDNA isolated from 20-30 pooled embryos per timepoint. Error bars indicate s.e.m. of three biological samples. (B-G) Whole-mount *in situ* hybridization (WISH) of *gata2b* expression at the indicated stages. Yellow arrowheads indicate expression in the vascular cord region (C) and dorsal aorta (DA) (D,E). Blue arrowheads indicate branchiomotor neurons (D-F). Pink arrowheads indicate expression in the caudal hematopoietic tissue (CHT) (F,G). (H) qPCR of *gata2b* expression in GFP$^+$ cells isolated from *fli1a:GFP* embryos by FACS. n.d., not detected. GFP$^+$ cells sorted from 20-30 pooled embryos per timepoint. Error bars indicate s.e.m. of three technical replicates. (I) Transverse trunk sections showing WISH for *gata2b* at 18 hpf. Top, rare cell detected outside the midline (asterisk). Bottom, representative section with *gata2b*$^+$ cell localized to the midline. (J-M) Transverse sections showing WISH for *gata2b* (J), *runx1* (K), *kdrl* (L) and *gata2a* (M) at 25 hpf. Pink dashed ovals indicate the DA; orange dashed ovals indicate the posterior cardinal vein (PCV). Yellow arrowhead indicates a primitive erythrocyte. (N) Quantitation of *gata2a* and *gata2b* transcripts in *kdrl*$^+$ *cmyb*$^-$ and *kdrl*$^+$ *cmyb*$^+$ cells from 36 hpf and 48 hpf *kdrl:mCherry*^{mem}*;cmyb:GFP* embryos. Cells isolated from 50-100 pooled embryos per sample. Two biological experiments were performed for each timepoint, with one representative shown. Error bars indicate s.e.m. of three technical replicates for each representative experiment.

(Fig. 2C, arrowheads). No expression was detected in this region at 16 hpf, indicating that expression of *gata2b* at the midline initiated between 16 and 18 hpf (Fig. 2B,C). By 20 hpf, *gata2b* is expressed in the DA (Fig. 2D, yellow arrowheads), as well as in branchiomotor neurons (Fig. 2D, blue arrowheads). At 50 and 72 hpf, *gata2b* expression can be observed in hematopoietic cells within the CHT region (Fig. 2F,G, pink arrowheads).

To investigate whether *gata2b*-expressing cells at the midline at 18 hpf are from the PLM, we sorted cells positive for *fli1a:EGFP*, which marks the PLM and the hematovascular cells that it gives rise to (Lawson and Weinstein, 2002; Thompson et al., 1998). In line with our *gata2b* WISH analysis, we did not detect *gata2b* by qPCR at 16 hpf in *fli1a*$^+$ cells, but detected expression in this tissue from 18 to 26 hpf (Fig. 2H). To determine *gata2b* expression with greater spatial precision, we transversely sectioned the embryonic trunk region. In 18-hpf embryos, *gata2b* expression was observed within the vascular cord, as well as in rare cells outside the midline, consistent with initiation near the end of PLM convergence (Fig. 2I). At 25 hpf, transverse trunk sections showed *gata2b* expression in an endothelial subpopulation polarized to the ventral wall of the aorta, similarly to *runx1* (Fig. 2J,K), whereas *gata2a* was detected throughout the DA and posterior cardinal vein (PCV), similarly to the vascular marker *kdrl*, as well as in primitive erythrocytes (Fig. 2L,M). In conclusion, although both *gata2a* and *gata2b* are expressed in the DA, they have distinctly different expression patterns within this tissue.

Next, we examined *gata2b* expression within hemogenic endothelium. By combining fluorescent reporter animals that mark vasculature (*kdrl:mCherry*^{mem}) or hematopoietic cells (*cmyb:GFP*), nascent HSPCs (*kdrl:mCherry*$^+$*;cmyb:GFP*$^+$) can be distinguished from vascular, non-hemogenic endothelium (*kdrl:mCherry*$^+$*;cmyb:GFP*$^-$) at 36 hpf (Bertrand et al., 2010). At 36 hpf, *gata2a* is enriched within vascular endothelium as compared with nascent

Development (2015) 142, 1050-1061 doi:10.1242/dev.119180

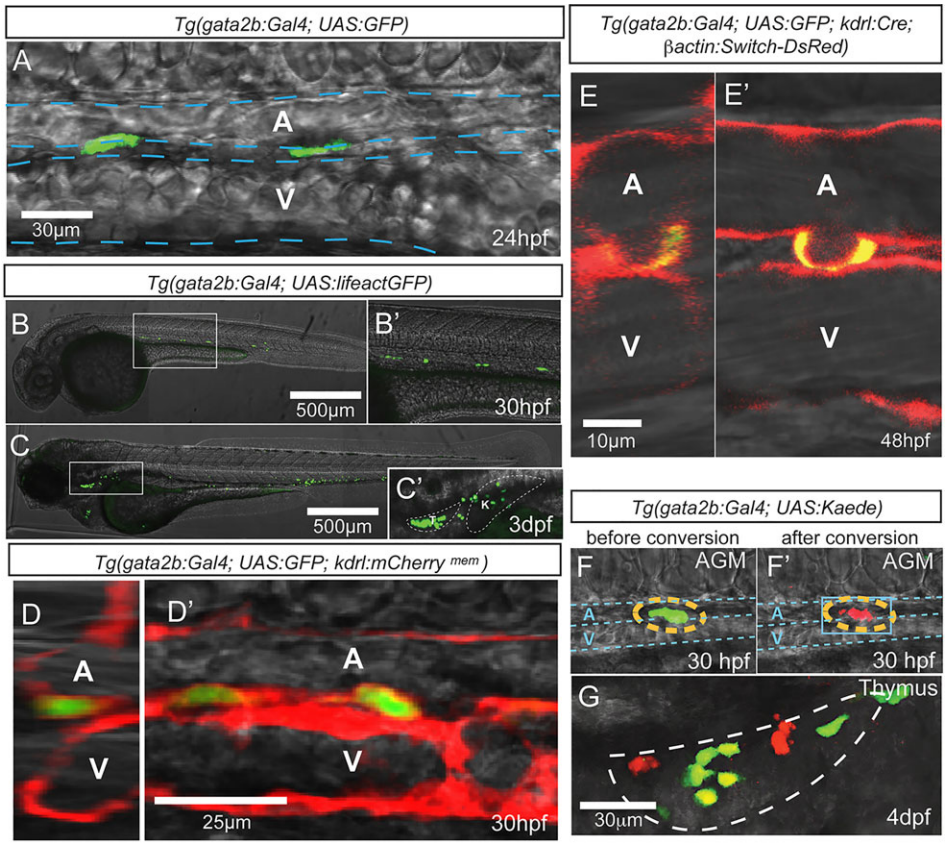

Fig. 3. *Tg(gata2b:Gal4)* marks hemogenic endothelial cells. Imaging is by confocal microscopy. (A) GFP$^+$ endothelial cells in the trunk region of a *gata2b:Gal4;UAS:GFP* embryo at 24 hpf. (B-C′) *gata2b:Gal4;UAS:lifeactGFP* at 30 hpf and 3 dpf. (C′) An enlarged view of C, with thymus and kidney highlighted. (D,D′) Transverse (D) and lateral (D′) views of the trunk vasculature of 30 hpf *gata2b:Gal4;UAS:GFP;kdrl:mCherry^{mem}*. (E,E′) Transverse (E) and lateral (E′) views of a 48 hpf *gata2b:Gal4;UAS:GFP;kdrl:Cre;actB2:LoxP-STOP-LoxP-DsRedEx* embryo showing a GFP$^+$ cell undergoing EHT. (F,F′) A representative Kaede$^+$ cell in the trunk of a *gata2b:Gal4;UAS:Kaede* embryo before (F) and after (F′) photoconversion. Blue dashed lines indicate the approximate location of DA and PCV. (G) Thymus of a 4 dpf *gata2b:Gal4;UAS:Kaede* embryo that experienced photoconversion of a single aortic *gata2b*$^+$ cell in the trunk at 46 hpf. White dashed line highlights the thymus region. T, thymus; K, kidney; A, aorta; V, vein.

HSPCs (Fig. 2N). Consistent with expression observed by WISH, *gata2b* expression is enriched within hematopoietic cells generated by the aortic endothelium (Fig. 2N). The specific expression and early initiation of *gata2b* make it of particular interest for studying mechanisms governing HSC specification prior to *runx1* initiation.

A *gata2b:Gal4* transgene marks hemogenic endothelium

To further characterize *gata2b* as a possible marker of hemogenic endothelium and nascent HSCs, we generated transgenic zebrafish reporting *gata2b* expression. As *gata2b* is expressed specifically but at a low level within hemogenic endothelium, we utilized the Gal4-*UAS* system to amplify expression. This system also creates flexibility, allowing a single transgenic *Gal4* driver line to be used in conjunction with a variety of *UAS*-driven effector lines. Using BAC recombineering (Bussmann and Schulte-Merker, 2011) and Tol2-mediated transgenesis, we created transgenic animals driving optimized *Gal4* (*KalTA4*) (Distel et al., 2009) under the control of *gata2b* regulatory elements. By crossing *gata2b:Gal4* to Gal4-responsive fluorescent reporters, including *UAS:GFP* and *UAS:lifeactGFP*, we observed GFP fluorescence at 24 hpf in cells with a flattened morphology in the aortic floor region (Fig. 3A). At 30 hpf, GFP expression was consistent with the hematopoietic expression of *gata2b* as assessed by WISH, although no fluorescence was observed in branchiomotor neurons (Fig. 3B). By 3 days post-fertilization (dpf), *gata2b:Gal4;UAS:lifeactGFP* fluorescence remained restricted to hematopoietic populations in the CHT, thymus and kidney, with round hematopoietic cells also observed in association with the heart lumen (Fig. 3C; supplementary material Movie 1). This indicates that *gata2b:Gal4* drives expression specifically in cells at sites of HSC emergence and colonization (CHT, thymus and kidney). By contrast, *gata2a:GFP* shows GFP expression in the DA, PCV, primitive erythrocytes and spinal cord neurons, consistent with endogenous *gata2a* expression observed by WISH (supplementary material Fig. S1).

Our data suggested that *gata2b:Gal4* drives expression in hemogenic endothelial cells. Hemogenic endothelial cells are integral to the aortic wall (Bertrand et al., 2010; Chen et al., 2011; de Bruijn et al., 2002; Jaffredo et al., 1998; North et al., 1999) and undergo a characteristic morphological change during EHT (Kissa and Herbomel, 2010). To determine whether *gata2b*$^+$ cells in *gata2b:Gal4* animals behave in a similar way, we analyzed *gata2b:Gal4* in the context of the pan-vascular marker *kdrl*. In *gata2b:Gal4;UAS:GFP;kdrl:mCherry^{mem}* embryos, GFP$^+$ cells co-express the vascular marker *kdrl:mCherry^{mem}*, indicating that they are indeed within the aortic endothelium (Fig. 3D). Furthermore, *gata2b:Gal4*-driven expression marked cells undergoing the stereotypical budding characteristic of EHT (Kissa and Herbomel, 2010) (Fig. 3E). Using time-lapse imaging, we visualized the emergence of GFP$^+$ cells from the endothelium (supplementary material Movie 2).

Following EHT, HSPCs migrate to the CHT for amplification and differentiation, before homing to the thymus, which is the primary site of T-cell development (Bertrand et al., 2008; Kissa et al., 2008; Murayama et al., 2006; Zhang et al., 2011). In *gata2b:Gal4;UAS:lifeactGFP* fish, we observed *gata2b*$^+$ cells first in the aortic floor and later in the thymus (Fig. 3B,C). By photoconverting *gata2b*$^+$ cells in *gata2b:Gal4;UAS:Kaede* fish, we traced cells from the aorta at 46 hpf to the thymus at 4 dpf, confirming that GFP$^+$ thymic cells derive from *gata2b*$^+$ hemogenic endothelial cells (Fig. 3F,G). Moreover, thymic *gata2b*$^+$ cells coexpressed the T-cell marker *lck:nls-mCherry* at 4 dpf (supplementary material Fig. S2), indicating that *gata2b*$^+$ cells have lymphoid potential.

Together, these data indicate that *gata2b*-expressing cells first reside within the DA, later emerging through EHT to migrate to the CHT, thymus and embryonic kidney. Furthermore, *gata2b*$^+$ cells

Development (2015) 142, 1050-1061 doi:10.1242/dev.119180

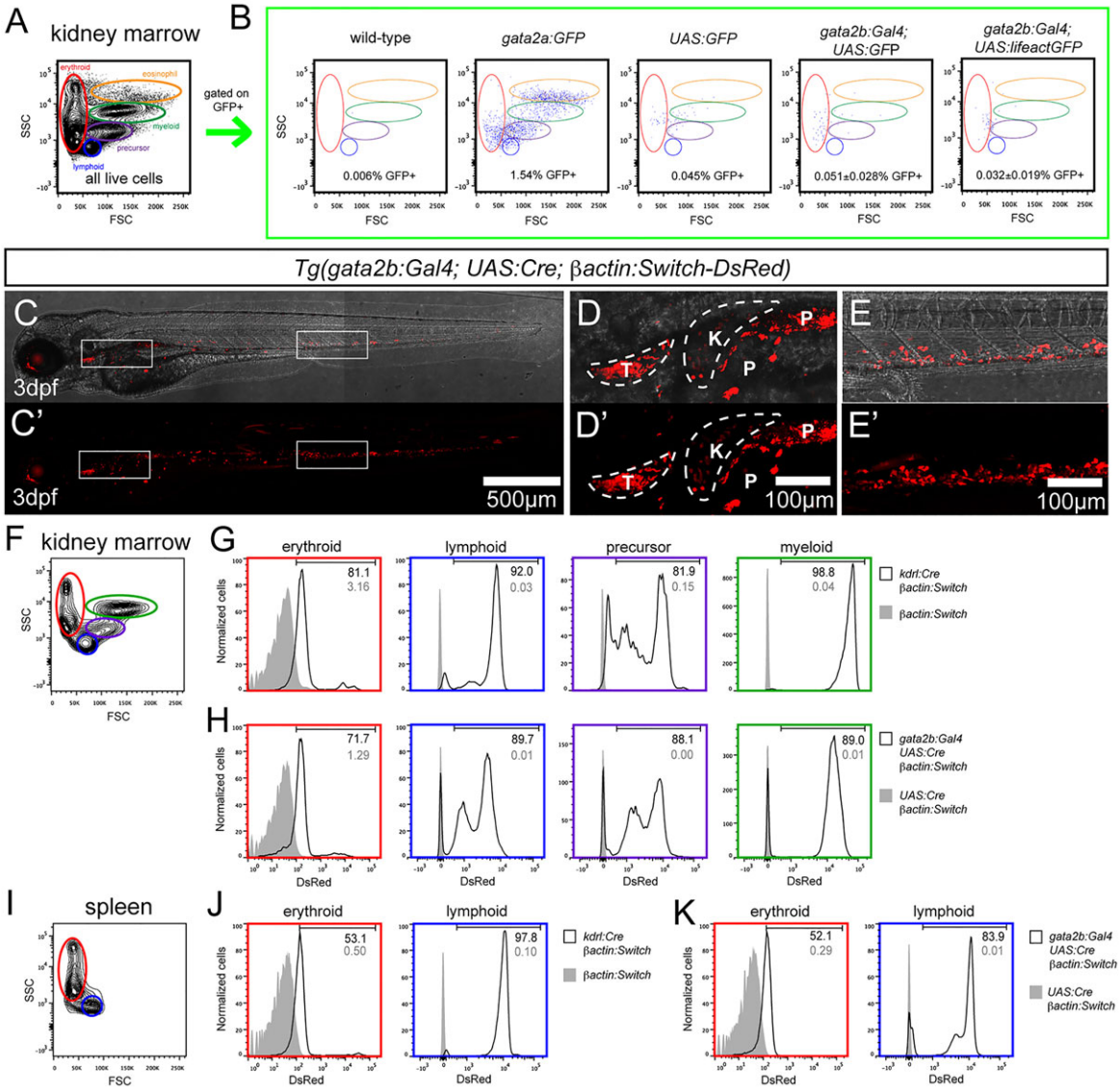

Fig. 4. *gata2b*$^{+}$ cells give rise to adult blood. (A,B) Analysis of GFP^{+} cells in the whole kidney marrow (WKM). (A) Representative flow cytometry analysis of the adult WKM, including the distribution of erythroid (red), lymphoid (blue), precursor (purple), myeloid (green) and eosinophil (orange) populations. (B) Percentage and distribution of GFP^{+} cells from the WKM of adult zebrafish of the indicated genotypes. Scatter plots depict the forward and side scatter distribution of GFP^{+} cells from the WKM, with populations marked as in A for reference. For wild type (*n*=1), *gata2a:GFP* (*n*=2) and *UAS:GFP* (*n*=2), the indicated percentage corresponds to the representative scatter plot. For *gata2b:Gal4;UAS:GFP* (*n*=3) and *gata2b:Gal4;UAS:lifeactGFP* (*n*=3), a representative scatter plot is shown and the indicated percentage of GFP^{+} cells corresponds to the average±s.d. (C-E′) *gata2b:Gal4;UAS:Cre;βactin:Switch-DsRed* embryo at 3 dpf. (C,C′) DsRed fluorescence in the whole embryo. (D,D′) Enlarged view of thymus (T) and kidney (K) region from C,C′; P, pigment. (E,E′) Enlarged view of the CHT region from C,C′. (F) Representative flow cytometry analysis of adult WKM. (G) DsRed fluorescence of erythroid, lymphoid, precursor and myeloid fractions of WKM of *βactin:Switch-DsRed* (gray filled) and *kdrl:Cre;βactin:Switch-DsRed* (black line). (H) DsRed fluorescence of erythroid, lymphoid, precursor and myeloid fractions of WKM of *UAS:Cre;βactin:Switch-DsRed* (gray filled) and *gata2b:Gal4;UAS:Cre;βactin:Switch-DsRed* (black line). (I) Representative flow cytometry analysis of the adult spleen. (J) DsRed fluorescence of erythroid and lymphoid fractions of the spleen of *βactin:Switch-DsRed* (gray filled) and *kdrl:Cre;βactin:Switch-DsRed* (black line). (K) DsRed fluorescence of erythroid and lymphoid fractions of the spleen of *UAS:Cre;βactin:Switch-DsRed* (gray filled) and *gata2b:Gal4;UAS:Cre;βactin:Switch-DsRed* (black line). (G,H,J,K) Numbers indicate percentage of cells in the DsRed^{+} fraction.

have lymphoid potential, suggesting that they might be early HSPCs.

gata2b^{+} cells give rise to adult hematopoietic cells

Nascent HSCs seed the kidney, where they amplify and are maintained during adult homeostasis, and differentiate into erythroid, lymphoid and myeloid lineages. Erythroid, lymphoid, myeloid and hematopoietic precursor cells within the adult whole kidney marrow (WKM) can be separated by flow cytometry based upon light scatter characteristics (Traver et al., 2003). In adult zebrafish, *gata2a:GFP* is expressed in the kidney marrow, where it primarily labels eosinophils (Balla et al., 2010; Traver et al., 2003). By contrast, *gata2b:Gal4* does not drive fluorescence in the adult kidney marrow when combined with either *UAS:GFP* or *UAS:lifeactGFP* (Fig. 4A,B).

Permanent genetic labeling of endothelial cells and their derivatives with endothelial-specific *kdrl:Cre* in combination with the lineage marker *actB2:LoxP-STOP-LoxP-DsRedEx* has indicated that embryonic hemogenic endothelium is the origin of zebrafish adult blood cells (Bertrand et al., 2010). In this lineage-tracing

Development (2015) 142, 1050-1061 doi:10.1242/dev.119180

approach, *actB2:LoxP-STOP-LoxP-DsRedEx* (also known as *βactin:Switch-DsRed*) undergoes excision of the STOP cassette in *Cre*-expressing cells, resulting in a permanent 'switch' from non-fluorescence to DsRed$^+$ for these cells and their progeny. To investigate whether *gata2b*$^+$ cells have the potential to give rise to the adult hematopoietic system, we performed lineage tracing in *gata2b:Gal4;UAS:Cre;βactin:Switch-DsRed* zebrafish. As expected, DsRed fluorescence marked cells in the CHT, thymus and kidney in 3 dpf embryos (Fig. 4C-E), closely resembling *gata2b:Gal4;UAS:lifeactGFP* embryos at this time (Fig. 3C). Whereas *gata2b:Gal4* initially drives expression in the DA, we did not detect *gata2b*$^+$ cells in the endothelium at 3 dpf (Fig. 3A,C).

To determine the contribution of *gata2b*$^+$ cells to adult blood, we analyzed DsRed$^+$ cells in the WKM by flow cytometry. Lineage tracing of the endothelium in *kdrl:Cre;βactin:Switch-DsRed* fish labeled the vast majority of hematopoietic cells within the WKM, with no DsRed$^+$ cells in the WKM of *βactin:Switch-DsRed* zebrafish alone (Fig. 4F,G). In comparison, within the WKM of 2-month post-fertilization *gata2b:Gal4;UAS:Cre;βactin:Switch-DsRed* fish, 87.8±1.8% of lymphoid cells, 84.8±7.0% of myeloid cells and 85.2±6.6% of precursor cells were DsRed$^+$ (n=3). Although we observed some leakiness of the *UAS:Cre* transgene within a small number of DsRed$^+$ muscle and neural cells in 3-dpf embryos, adult *UAS:Cre;βactin:Switch-DsRed* fish had less than 0.1% DsRed$^+$ cells in the lymphoid, myeloid and precursor fractions of the WKM (n=2) (Fig. 4H), indicating that *gata2b*$^+$ cells give rise to the majority of blood cells in the adult WKM in a multilineage manner. Similarly, switched DsRed$^+$ cells comprised the majority of the erythroid and lymphoid cells within the spleens of *kdrl:Cre;βactin:Switch-DsRed* (Fig. 4I,J) and *gata2b:Gal4;UAS:Cre;βactin:Switch-DsRed* (Fig. 4K) fish, whereas no labeling was observed in the spleens of *βactin:Switch-DsRed* or *UAS:Cre;βactin:Switch-DsRed* control animals. Using the *gata2b:Gal4* transgenic line, we have demonstrated that the majority of hematopoietic cells are derived from *gata2b*$^+$ cells.

Taken together, our data indicate that *gata2b* is expressed specifically within aortic hemogenic endothelium, which gives rise to the vast majority of adult hematopoietic cells.

gata2b is required for HSC formation

To establish whether *gata2b* is required for HSC development, we performed targeted knockdown of *gata2b* using a splice-blocking morpholino oligonucleotide (MO). This MO results in intron retention leading to missense sequence and a premature STOP codon before the zinc-finger domains (supplementary material Fig. S3), which is predicted to inhibit the DNA binding of Gata2b. Initially, *gata2b* morphants express normal levels of *etsrp* (*etv2* – ZFIN), *gata1a*, *scl* (*tal1* – ZFIN) and *runx1* within the PLM (supplementary material Fig. S4). Primitive hematopoiesis appears unaffected in *gata2b* morphants, with normal expression of *gata1a* and *scl* in primitive erythrocytes and *l-plastin* (*lcp1* – ZFIN) in primitive macrophages at 22 hpf (supplementary material Fig. S4I-N). In addition to having normal PLM and primitive hematopoiesis, *gata2b* morphants maintain normal somitic and pronephric duct development (supplementary material Fig. S4A-R), suggesting normal development of morphant embryos.

We next investigated whether *gata2b* is required for the formation of hemogenic endothelium and HSCs. One of the earliest known markers of HSC fate in zebrafish is the transcription factor *runx1* (Burns et al., 2002; Wilkinson et al., 2009). Knockdown of *gata2b* results in a decrease of *runx1* in the DA floor at 25 hpf, whereas a similar MO with five base-pair mismatches does not (Fig. 5A,B; supplementary material Fig. S3E,F). An ATG MO targeting the translation start site of *gata2b* phenocopies the reduction of *runx1* expression in the DA (supplementary material Fig. S3H). To further confirm the hemogenic endothelial defect in *gata2b* morphants, we assessed expression of the transcription factor *cmyb*, which is genetically downstream of *runx1* in hemogenic endothelial cells (Burns et al., 2005), and of *rag1*, a marker of lymphoid potential. Consistent with the loss of *runx1*, *cmyb* expression was reduced in *gata2b* morphants at 36 hpf (Fig. 5C,D). Similarly, *rag1*$^+$ thymocytes were severely reduced in *gata2b* morphants at 4 dpf (Fig. 5E,F), further indicating that *gata2b* is essential for the production of functional HSCs.

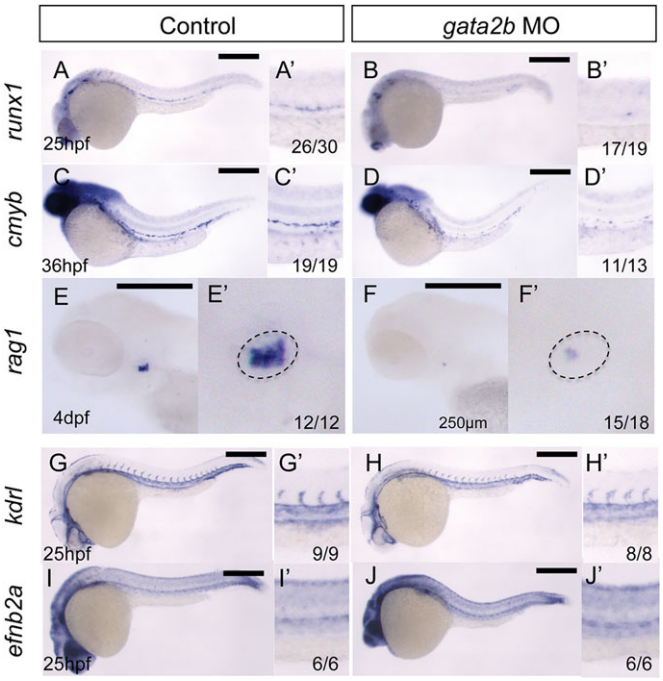

Fig. 5. *gata2b* is required for the formation of HSCs. (A-J) WISH of the indicated genes in wild-type embryos and *gata2b* morphant siblings at the stages indicated. (A′,B′,C′,D′,G′,H′,I′,J′) Magnified views of the trunk region. (E′,F′) Magnified views of the thymus region (dashed ovals) of E,F. The number of embryos showing the illustrated phenotype among the total examined is indicated. Scale bars: 250 μm.

Owing to the remarkable differences in endothelial *gata2a* and *gata2b* expression, we hypothesized that *gata2b* might have taken on a specialized role within the hemogenic endothelial compartment while *gata2a* has remained essential to vascular morphogenesis. Strengthening this hypothesis, depletion of *gata2b* did not affect the expression of *kdrl* or *efnb2a* (Fig. 5G-J), indicating normal vascular development and arterial specification. Importantly, circulation was normal in *gata2b* morphants (supplementary material Movies 3 and 4). By contrast, *gata2a*^{um27} mutants lack trunk circulation (Zhu et al., 2011) and experience hemorrhages (supplementary material Fig. S1), consistent with the consequences of vascular endothelial deletion of *Gata2* in mice (de Pater et al., 2013; Johnson et al., 2012; Lim et al., 2012).

We next tested whether the Gata2a and Gata2b proteins are functionally redundant by attempting to rescue *gata2b* morphants with ectopic expression of *gata2a* or *gata2b*. We found that *gata2b* successfully rescued *gata2b* splice morphants, whereas *gata2a* did not (supplementary material Fig. S3I-M), consistent with our hypothesis that Gata2a and Gata2b fulfill distinct requirements. Together, our results suggest that the requirement of GATA2 for endothelial integrity appears to be maintained by the zebrafish

Development (2015) 142, 1050-1061 doi:10.1242/dev.119180

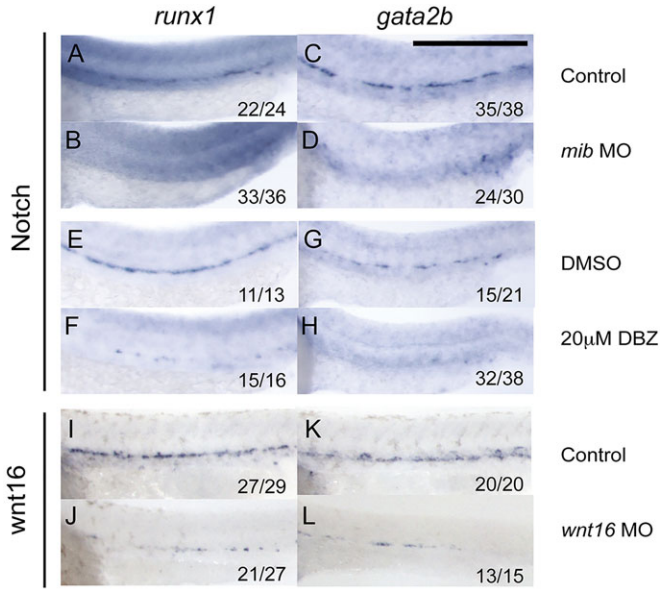

Fig. 6. Notch and non-canonical Wnt signaling contribute to *gata2b* expression in hemogenic endothelium. (A-D) WISH of *runx1* and *gata2b* expression in control and *mib* morphant siblings. (E-H) Expression of *runx1* and *gata2b* in embryos treated with DMSO or the γ-Secretase inhibitor DBZ from 10 to 24 hpf. (I-L) Expression of *runx1* and *gata2b* in control and *wnt16* morphant siblings. Scale bar: 250 μm.

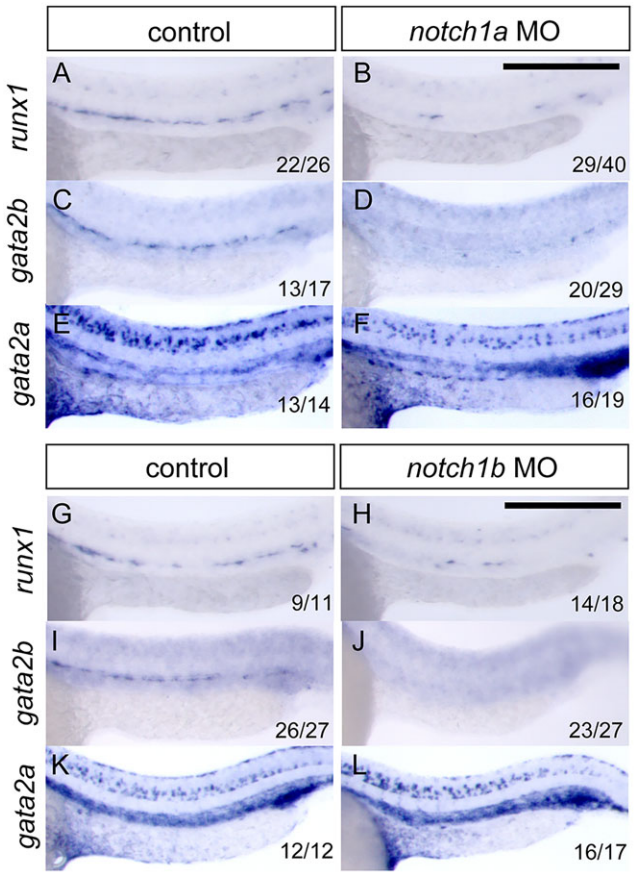

Fig. 7. *notch1a* and *notch1b* are required for expression of *gata2b*, but not *gata2a*, within the endothelium. (A-F) Expression of *runx1* (A,B), *gata2b* (C,D) and *gata2a* (E,F) in control and *notch1a* morphant siblings. (G-L) Expression of *runx1* (G,H), *gata2b* (I,J) and *gata2a* (K,L) in control and *notch1b* morphant siblings. Scale bars: 250 μm.

Gata2a paralog, whereas Gata2b serves a specialized role within hemogenic endothelium.

Notch signaling is required for hematopoiesis through its upstream regulation of *Runx1* (Nakagawa et al., 2006). In zebrafish, Notch signaling is required for aortic *cmyb* expression, and *cmyb* loss as a result of Notch inhibition can be rescued by *runx1* mRNA injection (Burns et al., 2005). To determine where Gata2b functions in this pathway, we tested whether ectopic *runx1* could rescue *cmyb* expression in *gata2b* morphants. Co-injection of *gata2b* MO with *runx1* mRNA was sufficient to rescue the loss of *cmyb* in hemogenic endothelium (supplementary material Fig. S3N-Q), indicating that *gata2b* is required upstream of *runx1* in hemogenic endothelium.

gata2b is regulated by Notch signaling

Both cell-autonomous and non-cell-autonomous Notch signaling is required for the formation of vertebrate HSCs (Hadland et al., 2004; Kim et al., 2014). Notch signaling is required for both arterial specification and HSC formation from arterial vasculature. *Gata2* is a direct Notch target in the mouse DA (Robert-Moreno et al., 2005) and is regulated by hematopoietic, rather than arterial, Notch signaling (Robert-Moreno et al., 2008). Somitic Wnt16 is required upstream of both somite-intrinsic and somite-to-PLM Notch signaling without affecting arterial specification (Clements et al., 2011; Kim et al., 2014; Kobayashi et al., 2014), demonstrating that the Notch requirements of arterial and HSC development are separable in zebrafish. Surprisingly, *gata2a* expression in the aortic endothelium is unaffected by knockdown of *wnt16* (Clements et al., 2011), which led us to investigate whether Notch signaling is required for the expression of *gata2b* in hemogenic endothelium.

We first performed inhibition of Notch signaling in the whole embryo. The E3 ubiquitin ligase Mindbomb (Mib) is required for functionality of the Notch ligand on the signal-emitting cell (Itoh et al., 2003). Knockdown of Notch signaling using a *mib* MO resulted in downregulation of both *runx1* and *gata2b* (Fig. 6A-D). This finding was recapitulated by chemical inhibition of γ-Secretase, which prevents release of the transcriptionally active intracellular domain from the membrane-bound Notch receptor (Mumm et al., 2000). Treatment with the γ-Secretase inhibitor dibenzazepine (DBZ) (Milano et al., 2004; van Es et al., 2005) from 10 hpf resulted in downregulation of both *runx1* and *gata2b* in the DA (Fig. 6E,H). Furthermore, knockdown of *wnt16*, which functions upstream of the Notch signaling required for HSC formation, resulted in the reduction of both *runx1* and *gata2b* in the DA (Fig. 6I-L), suggesting that Notch regulates zebrafish *gata2b* in a similar manner to murine *Gata2*.

Three of the four Notch receptors are necessary for *runx1* expression in zebrafish but function in different tissues (Kim et al., 2014). The NOTCH1 homologs Notch1a and Notch1b act directly within endothelial cells, whereas Notch3 is dispensable within the endothelium but required in the somite via an unknown mechanism (Kim et al., 2014). Because *Gata2* is a direct NOTCH1 target in the murine DA (Robert-Moreno et al., 2005), we examined whether the receptors required within the endothelium function upstream of *gata2b*. Individual knockdowns of *notch1a* and *notch1b* resulted in decreased *runx1* and *gata2b* expression (Fig. 7A-D,G-J). By contrast, expression of *gata2a* was unaffected by loss of either receptor (Fig. 7E, F,K,L). The endothelial Notch signaling that is required for the hemogenic capacity of the DA thus regulates *gata2b* but not *gata2a*.

Together, our results demonstrate that *gata2b* is expressed in early hemogenic endothelium, where it is required upstream of *runx1* to

Development (2015) 142, 1050-1061 doi:10.1242/dev.119180

determine HSC fate. In addition, *gata2b* is regulated by the Notch receptors that function specifically within the endothelium to promote hematopoiesis, whereas *gata2a* is not. These data suggest that, following duplication of the ancestral *gata2* gene, subfunctionalization of each paralog has resulted in *gata2b* regulating HSC emergence.

DISCUSSION

Subfunctionalization of Gata2a and Gata2b in zebrafish

The division of labor between duplicated genes to recapitulate the functions of the ancestral gene is known as subfunctionalization (Force et al., 1999). Genome duplication within the teleost lineage has yielded two Gata2 paralogons that have been maintained in these jawed, bony, ray-finned fish, including medaka, fugu (pufferfish), *Tetraodon*, stickleback and zebrafish (Gillis et al., 2009). We demonstrate a divergence in the expression patterns of *gata2a* and *gata2b* in zebrafish, with *gata2a* expressed throughout the endothelium and *gata2b* restricted to the hemogenic subpopulation of the DA. Despite both being expressed in the endothelium, *gata2a* and *gata2b* have a high level of sequence divergence and are regulated differently, suggesting that they might have divergent functions within the embryonic endothelium. Accordingly, *gata2a* is required for endothelial integrity and vascular morphogenesis (Zhu et al., 2011), whereas *gata2b* is required in an HSC-specific manner. During mouse embryogenesis, GATA2 is required in the endothelium for both the maintenance of endothelial integrity and HSC formation (de Pater et al., 2013; Johnson et al., 2012; Lim et al., 2012). Together, Gata2a and Gata2b appear to additively fulfill the endothelial roles of GATA2, suggesting that duplication of the *gata2* locus has led to an evolutionary separation of its endothelial and hematopoietic functions.

The zinc-finger domains of GATA2 that mediate DNA binding and interaction with transcriptional partners (Vicente et al., 2012) are largely conserved between zebrafish Gata2a and Gata2b and the human and mouse GATA2 proteins. Outside this region the proteins are more divergent, and it is not clear which regions are responsible for the different functions performed by Gata2a and Gata2b. In mice, GATA2 can inhibit the production of $CD45^+$ cells from the aorta-gonad-mesonephros (AGM) region (Minegishi et al., 2003). The domain responsible for this activity, comprising amino acids 75-235, has transcriptional repressive activity in the GATA2 protein; however, a partially conserved region in GATA3 acts as a transcription activation domain (Minegishi et al., 2003; Yang et al., 1994). It is possible that differences in this domain might explain distinct activities of the Gata2a and Gata2b proteins. Future functional comparisons of Gata2a and Gata2b with human and mouse GATA2 might yield a greater understanding of the roles that Gata2 plays in different endothelial and hematopoietic contexts.

Expression of *gata2b* marks early hemogenic endothelium

The process by which endothelial cells acquire hemogenic capacity has not been fully resolved. Understanding when and how this occurs during embryogenesis can inform future efforts to derive these cells *in vitro*. HSCs emerge from ventral endothelium of the DA (Bertrand et al., 2010; Boisset et al., 2010; Chen et al., 2009; Kissa and Herbomel, 2010; Lam et al., 2010; Taoudi and Medvinsky, 2007). Several signaling pathways, including Hedgehog, VEGF and multiple Notch inputs, are important for the formation of hemogenic endothelium upstream of *runx1* expression (Gering and Patient, 2005; Kim et al., 2014). Owing to a paucity of markers for the early detection of hematopoietic specification within endothelium, we lack a full understanding of how these cues drive the establishment of HSC fate.

The markers that distinguish hemogenic endothelium from arterial endothelium, including *runx1*, *cmyb* and *cd41* (*itga2b* – ZFIN), have only been observed in the endothelium following formation of the DA. It is now evident that specification of both arterial and hemogenic endothelium begins earlier than previously postulated. In particular, migrating PLM cells appear to adopt arterial or venous fate well before formation of the vascular cord (Hong et al., 2006; Kohli et al., 2013; Quillien et al., 2014), with arterial specification beginning within the PLM as early as 11 hpf, at the 5-somite stage (Quillien et al., 2014). Somitic Notch ligands DeltaC and DeltaD downstream of Wnt16 are required for the formation of hemogenic endothelium (Clements et al., 2011), and these ligands activate Notch signaling in the PLM during migration to the midline between 14 and 18 hpf (Kobayashi et al., 2014). When this signal is missing, arterial specification is unaffected but hemogenic endothelium is lost (Kobayashi et al., 2014). As we observe that the expression of *gata2b* initiates in a small population of *fli1a*$^+$ cells just before and during formation of the vascular cord at 18 hpf, it is plausible that Notch signaling from the somite initiates *gata2b* expression to prime the HSC program.

Regulation of *gata2b* expression

Notch signaling regulates HSC formation through both direct and indirect mechanisms (Clements et al., 2011; Hadland et al., 2004; Kim et al., 2014; Kobayashi et al., 2014). Our data demonstrate that Notch signaling is required for the expression of *gata2b* in hemogenic endothelium. In mouse, both GATA2 and NOTCH1 are required cell-autonomously for formation of HSCs (Hadland et al., 2004; Tsai et al., 1994). The transcriptionally active NOTCH1 intracellular domain (NICD1) associates with the *Gata2* promoter in the mouse embryo at E9.5, just before HSC emergence, and is required for *Gata2* expression in the DA (Guiu et al., 2013; Robert-Moreno et al., 2005). These findings suggest that *Gata2* is a direct target of a cell-autonomous Notch signal within hemogenic endothelium. In zebrafish, the Notch1a and Notch1b receptors are required specifically within the endothelium for HSC formation (Kim et al., 2014). Our data demonstrate that Notch1a and Notch1b are required for *gata2b*, but not *gata2a*, in the DA, suggesting that there might be a conserved role of endothelial Notch signaling in the regulation of *gata2b* in zebrafish.

RUNX1 is required cell-intrinsically within hemogenic endothelium for HSC formation (Chen et al., 2009). Expression of *Runx1* in the DA is dependent upon Notch signaling in both mice and zebrafish (Burns et al., 2005; Robert-Moreno et al., 2005). The hematopoietic defect in the absence of Notch signaling can be rescued by artificial induction of *Runx1* in cell culture (Nakagawa et al., 2006). Similarly, the hematopoietic defect resulting from Notch deficiency can be partially rescued through provision of exogenous *runx1* mRNA in zebrafish (Burns et al., 2005), indicating that Notch is required for HSC formation upstream of *runx1* activation in hemogenic endothelium. In our study, the hematopoietic defect of *gata2b* morphants is partially rescued by provision of *runx1* mRNA, suggesting that loss of *runx1* accounts for the hematopoietic phenotype observed with *gata2b* knockdown. Hemogenic endothelial expression of *Runx1* is governed by an intronic enhancer element that contains consensus sites for Runx, Cmyb, Gata, ETS and E-box transcription factors (Bee et al., 2009; Nottingham et al., 2007), but not for the Notch partner RBPjκ, suggesting that Notch signaling might be required through the induction of intermediate transcription factors to promote *Runx1* expression in hemogenic endothelium. The GATA binding site is crucial for the activity of this enhancer (Nottingham et al., 2007). Dysregulation of *Gata2* in the endothelium results in a reduction in *Runx1* expression in the AGM region (Gao et al., 2013). In this study we report a similar reduction in *runx1* expression in the DA with *gata2b* knockdown, indicating a conserved requirement for Gata2 within hemogenic endothelium.

Development (2015) 142, 1050-1061 doi:10.1242/dev.119180

The *gata2b:Gal4* transgene as a tool for future hematopoiesis studies

The *gata2b:Gal4* driver marks hemogenic endothelium and nascent HSCs from the DA to the CHT, thymus, pronephros and adult kidney. To our knowledge, *gata2b:Gal4* is the earliest, most specific marker of aortic hemogenic endothelium, allowing the direct visualization of hemogenic endothelium from as early as 24 hpf. In the future, this transgenic driver will prove useful in the unambiguous detection and tracking of hemogenic endothelial cells and HSCs. Because this line drives *Gal4* rather than a fluorescent protein, it can be used in conjunction with the growing number of UAS-driven transgenes. Furthermore, we have shown that *gata2b:Gal4;UAS:Cre;βactin:Switch-DsRed* effectively labels endothelial-derived blood until adulthood in a multilineage manner, demonstrating that *gata2b* is expressed in HSCs. With the increasing ease of genetic manipulation using the CRISPR/Cas9 system in zebrafish (Auer et al., 2014), *gata2b:Gal4;UAS:Cre* might ultimately prove most useful for the hematopoiesis-specific disruption of genes, such as *gata2a*, whose mutation results in developmental defects and embryonic lethality, but might serve unappreciated roles in the developing hematopoietic system.

MATERIALS AND METHODS

Zebrafish husbandry and maintenance

Zebrafish (*Danio rerio*) were maintained according to the guidelines of the UCSD Institutional Animal Care and Use Committee. The following zebrafish lines have been described previously: *Tg(fli1a:GFP)^{y1}* (Lawson and Weinstein, 2002), *Tg(kdrl:Has.HRAS-mCherry)^{s896}* (Chi et al., 2008), *Tg(cmyb:EGFP)^{zf169}* (North et al., 2007), *Tg(-20.7gata2:EGFP)^{la3}* (Traver et al., 2003), *Tg(4xUAS:GFP)^{hzm3}* (Distel et al., 2009), *Tg(UAS:lifeactGFP)^{mu271}* (Helker et al., 2013), *Tg(UAS:Kaede)^{rk8}* (Hatta et al., 2006), *Tg(actb2:loxP-STOP-loxP-DsRed)^{sd5}*(Bertrand et al., 2010), *gata2a^{um27}* (Zhu et al., 2011), *Tg(lmo2:GFP)^{zf72}* (Zhu et al., 2005), *Tg(gata1:DsRed)^{sd2}* (Traver et al., 2003) and *Tg(rag2:GFP)^{zdf8}* (Langenau et al., 2003). For clarity, throughout the text *Tg(kdrl:Has.HRAS-mCherry)^{s896}* is referred to as *kdrl:mCherry^{mem}*; *Tg(-20.7gata2:EGFP)^{la3}* is referred to as *gata2a:GFP*; *Tg(4xUAS:GFP)^{hzm3}* is referred to as *UAS:GFP*; *Tg(actb2:loxP-STOP-loxP-DsRed)^{sd5}* is referred to as *βactin:Switch-DsRed*; *TgBAC(gata2b:KalTA4)^{sd32}* is referred to as *gata2b:Gal4*; and *Tg(UAS:Cre,CY)^{zd17}* is referred to as *UAS:Cre*.

Whole-mount *in situ* hybridization (WISH)

Embryos were treated with 1-phenyl 2-thiourea (PTU) and fixed in 4% paraformaldehyde (Sigma-Aldrich) overnight at 4°C, then dehydrated and stored in methanol prior to staining. WISH was performed as described (Thisse et al., 1993). *In situ* hybridization probes were synthesized using the DIG RNA Labeling Kit (Roche). Hybridization probes were prepared as described for *gata1a* (Detrich et al., 1995), *gata2a* (Detrich et al., 1995), *scl* (Liao et al., 1998), *runx1* (Burns et al., 2005), *cmyb* (Thompson et al., 1998), *kdrl* (Thompson et al., 1998), *l-plastin* (Herbomel et al., 1999), *efnb2a* (Lawson and Weinstein, 2002), *cdh17*, *myod* (*myod1*), *etsrp* and *rag1* (Clements et al., 2011). Hybridization probe for zebrafish *gata2b* was synthesized from pExpress1-*gata2b* (IMAGE: 7037467; ATCC) linearized with *Eco*RV and transcribed using T7 RNA polymerase (Roche). For quantification of cells detected by WISH in the DA region, embryos with morphological defects that prevented reliable cell counting were excluded. Sections of embryos stained by WISH were embedded using the JB-4 Embedding Kit (Polysciences) and sectioned with a Leica RM2165 microtome at 7-9 µm thickness.

Fluorescence-activated cell sorting (FACS) and quantitative real-time PCR

For each sample, ∼50-100 embryos were stored on ice in 500 µl PBS with 2% FBS and were dissociated by pipetting. Cell suspensions were filtered using a 40-µm mesh and stained with SYTOX Red Cell Death Stain (Molecular Probes). Samples were sorted using a FACSAria IIu cell sorter (BD Biosciences). mRNA was isolated using the RNeasy Mini Kit (Qiagen). During mRNA extraction, 500 ng polyinosinic acid potassium salt (Sigma) was added to the RLT buffer for each sample. cDNA was synthesized using the Quantitect cDNA Synthesis Kit (Qiagen) according to the manufacturer's instructions. Quantitative PCR (qPCR) was performed using the BioRad CFX96 real-time system according to the manufacturer's instructions, with the following primers (5′-3′): gata2aQ-F, TCTTGAATCACTTGGACTCG; gata2aQ-R, GGACTGTGTATGAGGTGTGG; gata2bQ-F, ACCACCACACTCTGGAGAC; gata2bQ-R, CTGTTGCGTGTCTGAAT-ACC; ef1α (*eef1a1a* – ZFIN) primers have been previously described (Bertrand et al., 2007). Relative expression was calculated as $2^{[Ct(\text{gene of interest})-Ct(ef1\alpha)]}$. For quantification of *gata2a* and *gata2b* transcripts, an *in vitro* standard curve was generated by transfecting HEK cells with pCS2^{+}-*gata2a* or pCS2^{+}-*gata2b* plasmid.

Flow cytometry

Adult WKM samples were prepared as described (Traver et al., 2003), stained using SYTOX Red Cell Death Stain and analyzed using an LSRII flow cytometer (BD Biosciences).

gata2b MO design and validation

Antisense MOs were synthesized by Gene Tools. 1 nl MO solution was injected into single-cell embryos at the following concentrations: 30 mg/ml MO1-gata2b (*gata2b* splice acceptor MO) 5′-TTCACGTCCTATTGGCACACGATGC-3′; 30 mg/ml gata2b mismatch 5′-TTCACcTCgTATTcGCAgACcATGC-3′ (lowercase indicates mismatched nucleotides); 20 mg/ml MO2-gata2b (*gata2b* ATG MO) 5′-GGCATCCATCATCTCTCTTTTCAGT-3′. For MO validation, wild-type and morphant embryos were collected and mRNA was prepared using the RNeasy Mini Kit (Qiagen), and cDNA was prepared using SuperScript III reverse transcriptase (Invitrogen). RT-PCR was performed using primers (5′-3′): G2bEx3-F, CTGCTCGGAAACATGACGAC; G2bEx5-R, GTATAGACCGCAGGCATTGC. RT-PCR products were isolated using the QIAQuick Gel Extraction Kit (Qiagen). Purified PCR products were sequenced by Genewiz using primers G2bEx3-F (above) and G2bEx4-R (CTTGGGTCTGATGAGAGGTC). Sequences were analyzed using ApE software and sequence chromatograms were prepared using CodonCode Aligner.

Generation of expression constructs

To generate the pCMV6-*gata2b* construct, *gata2b* was amplified from 1- to 2-cell stage zebrafish embryo cDNA using Phusion polymerase (New England BioLabs) and primers (5′-3′): gata2b-F, TCGGCATCCCTGTCCTACTG; gata2b-R, GTCTCTCAGCCTATAGCAGTGAC. The PCR product was ligated into pCR-BluntII-Topo using the Zero Blunt Topo PCR Cloning Kit (Life Technologies). The *gata2b* cDNA fragment was subcloned into pCMV6-AC-Myc-His (OriGene) using *Bam*HI and *Xho*I (New England BioLabs). The pCS2-*gata2a-2A-tdTomato* construct was made using Multisite Gateway cloning (Life Technologies). *gata2a*, excluding the STOP codon, was amplified by PCR from 2-dpf embryo cDNA using the primers (5′-3′): Attb1-gata2a-F, GGGGACAAGTTTGTACAAAAAAGCAGGCTCCGCCACCATGGAGGTTGCGGCCGATCAG; Attb2r-gata2a-R(no-stop), GGGGACCACTTTGTACAAGAAAGCTGGGTGGTGTGGTTCGGCCCAGGCGGG. The resulting fragment was cloned into pDONR221 by BP reaction, generating pME-*gata2a(no stop)*. *2A-tdTomato* was amplified from pCS2-TAG (Addgene, 26772) using primers (5′-3′): Attb2-2A-tomato-F, GGGGACAGCTTTCTTGTACAAAGTGGACGGATCCGGAGCCACGAACTTCTCTCTGTTAAAGCAAGCAGGAGACGTGGAAGAAAACCCCGGTCCTATGGTGAGCAAGGGCGAGGAGG; Attb3r-tomato-R, GGGGACAACTTTGTATAATAAAGTTGGTTACTTGTACAGCTCGTCCATGCCG. The resulting PCR product was cloned to 3′ entry vector using BP recombination to produce p3E-*2A-tdTomato*. Subsequently, an LR reaction was performed using pME-*gata2a(no stop)*, p3E-*2A-tdTomato* and pCS-*Dest2* to create the final assembly of pCS2-*gata2a-2A-tdTomato*.

MO, plasmid and mRNA microinjection

For all MO, plasmid and mRNA microinjections, 1 nl was injected into 1- to 2-cell-stage zebrafish embryos. For previously published MOs, the

Development (2015) 142, 1050-1061 doi:10.1242/dev.119180

following concentrations were used: 5 mg/ml MO1-Mib (Itoh et al., 2003), 5 mg/ml Wnt16 MO (Clements et al., 2011), 10 mg/ml Notch1a-sp MO (Ma and Jiang, 2007) and 10 mg/ml Notch1b MO (Kim et al., 2014). For *runx1* mRNA rescue, *runx1* mRNA was synthesized from pCS2-*runx1* using the mMessage mMachine Kit (Life Technologies) and co-injected at 100 ng/µl. For plasmid rescue experiments, pCMV6-*gata2b* and pCSDest-*gata2a-2A-tdTomato* were injected at 20 ng/µl.

Generation of *TgBAC(gata2b:KalTA4)^{sd32}* zebrafish

The improved Gal4 variant KalTA4 (Distel et al., 2009) was inserted at the start codon of *gata2b* on the BAC CH211-157B11 (BACPAC Resources, Children's Hospital Oakland Research Institute, Oakland, CA, USA) using BAC recombineering as previously described (Bussmann and Schulte-Merker, 2011). The modified BAC was then injected together with *Tol2* mRNA into *Tg(4xUAS:GFP)^{hzm3}* zygotes (Distel et al., 2009). Transgenic fish were identified by mating to *Tg(4xUAS:GFP)^{hzm3}* and screening offspring for GFP expression.

Generation of *Tg(lck:nls-mCherry)^{sd31}* zebrafish

The *lck:nls-mCherry-CG2* transgenesis construct was created by Multisite Gateway recombination of p5′Entry-*lck-7.4 kb* (a kind gift from J. Yoder, North Carolina State University, Raleigh, NC, USA; Addgene, 58891), pME-*nls-mCherry* (Tol2kit #233), p3A-*polyA* (Tol2kit #302) and pDestTol2CG2 (Tol2kit #395). pDestTol2-*lck:nls-mCherry-CG2* was injected with *Tol2* mRNA (injection stock 25 ng/µl each; 1 nl total injection volume). *Tg(lck:nls-mCherry-CG2)* was first screened for GFP fluorescence in the heart. F1 *Tg(lck:nls-mCherry-CG2)* were crossed to *Tg(rag2:GFP)^{zdf8}* and *Tg(lck:lck-GFP)^{cz1}* to confirm localization of *nls-mCherry* to the correct cell types.

Generation of *Tg(UAS:Cre,CY)^{zd17}* zebrafish

pDestTol2*CY-UAS:Cre* (pCM339) features a UAS-controlled Cre recombinase ORF in a Tol2 transgenesis vector harboring *alpha-crystallin:YFP* as a transgenesis marker. The vector was assembled using Multisite Gateway cloning with the Tol2kit vector #327 (p5E-*UAS*), pDONR221-*Cre* and Tol2kit vector #302 (p3E-*SV40polyA*) into pDestTol2CY (pCM326) as backbone. pCM326 was cloned by ligating an *Asp*718I-flanked PCR product of *alpha-crystallin:YFP* (abbreviated *CY*) (Hesselson et al., 2009) into the *Asp*718I site in the Tol2kit backbone vector #394 (Kwan et al., 2007) in the same orientation as the Multisite Gateway cassette. *Tg(UAS:Cre,CY)^{zd17}* was generated by Tol2-mediated transgenesis, co-injecting 40 ng/µl pDestTol2*CY-UAS:Cre* (pCM339) plasmid and 20 ng/µl *Tol2* mRNA. *Tg(UAS:Cre,CY)^{zd17}* was first identified by YFP fluorescence in the lens at 3 dpf.

Confocal microscopy, time-lapse imaging and photoconversion

Embryos were mounted as previously described (Distel and Koster, 2007) and imaged using an SP5 inverted confocal microscope (Leica) as described (Bertrand et al., 2010). Images and time-lapse movies were created using Volocity software (PerkinElmer). Photoconversion was performed as described (Clements et al., 2011).

Acknowledgements

We thank Karen Ong, Jingjing Kobayashi-Sun, Clyde Campbell and Chase Melick for laboratory support; Roger Rainville for zebrafish care; Jeffrey Yoder for providing the *p5′Entry-lck-7.4 kb* plasmid; and Michiel van der Vaart and Stephanie Grainger for feedback on the manuscript.

Competing interests

The authors declare no competing or financial interests.

Author contributions

E.B., M.D., B.W., W.K.C. and D.T. designed experiments; E.B., K.N., C.-W.N. and N.D.L. generated expression constructs; M.D., E.B., C.M., F.E.P., A.M. and R.D. generated transgenic lines; E.B., M.D., C.P., B.W., I.K., D.L.S., K.N., N.D. and R.E.-P. performed research; E.B., M.D., B.W., C.P., N.D. and D.T. analyzed data; E.B. and D.T. wrote the paper with minor contributions from the remaining authors.

Funding

This work was supported by an American Heart Association (AHA) predoctoral fellowship [11PRE7580185 to E.B.]; EMBO fellowships (to M.D. and B.W.); a California Institute of Regenerative Medicine (CIRM) New Faculty Award [RN1-00575-1 to D.T.]; AHA Innovative Science Award [12PILT12860010 to D.T.]; and the National Institutes of Health [R01-DK074482 to D.T.]. Deposited in PMC for release after 12 months.

Supplementary material

Supplementary material available online at
http://dev.biologists.org/lookup/suppl/doi:10.1242/dev.119180/-/DC1

References

Auer, T. O., Duroure, K., De Cian, A., Concordet, J. P. and Del Bene, F. (2014). Highly efficient CRISPR/Cas9-mediated knock-in in zebrafish by homology-independent DNA repair. *Genome Res.* **24**, 142-153.

Balla, K. M., Lugo-Villarino, G., Spitsbergen, J. M., Stachura, D. L., Hu, Y., Banuelos, K., Romo-Fewell, O., Aroian, R. V. and Traver, D. (2010). Eosinophils in the zebrafish: prospective isolation, characterization, and eosinophilia induction by helminth determinants. *Blood* **116**, 3944-3954.

Bee, T., Ashley, E. L. K., Bickley, S. R. B., Jarratt, A., Li, P.-S., Sloane-Stanley, J., Gottgens, B. and de Bruijn, M. F. T. R. (2009). The mouse Runx1+23 hematopoietic stem cell enhancer confers hematopoietic specificity to both Runx1 promoters. *Blood* **113**, 5121-5124.

Bertrand, J. Y., Kim, A. D., Violette, E. P., Stachura, D. L., Cisson, J. L. and Traver, D. (2007). Definitive hematopoiesis initiates through a committed erythromyeloid progenitor in the zebrafish embryo. *Development* **134**, 4147-4156.

Bertrand, J. Y., Kim, A. D., Teng, S. and Traver, D. (2008). CD41+ cmyb+ precursors colonize the zebrafish pronephros by a novel migration route to initiate adult hematopoiesis. *Development* **135**, 1853-1862.

Bertrand, J. Y., Chi, N. C., Santoso, B., Teng, S., Stainier, D. Y. R. and Traver, D. (2010). Haematopoietic stem cells derive directly from aortic endothelium during development. *Nature* **464**, 108-111.

Boisset, J.-C., van Cappellen, W., Andrieu-Soler, C., Galjart, N., Dzierzak, E. and Robin, C. (2010). In vivo imaging of haematopoietic cells emerging from the mouse aortic endothelium. *Nature* **464**, 116-120.

Boisset, J. C., Clapes, T., Klaus, A., Papazian, N., Onderwater, J., Mommaas-Kienhuis, M., Cupedo, T. and Robin, C. (2014). Progressive maturation towards hematopoietic stem cells in the mouse embryo aorta. *Blood* **125**, 465-469.

Brown, L. A., Rodaway, A. R. F., Schilling, T. F., Jowett, T., Ingham, P. W., Patient, R. K. and Sharrocks, A. D. (2000). Insights into early vasculogenesis revealed by expression of the ETS-domain transcription factor Fli-1 in wild-type and mutant zebrafish embryos. *Mech. Dev.* **90**, 237-252.

Burns, C. E., DeBlasio, T., Zhou, Y., Zhang, J., Zon, L. and Nimer, S. D. (2002). Isolation and characterization of runxa and runxb, zebrafish members of the runt family of transcriptional regulators. *Exp. Hematol.* **30**, 1381-1389.

Burns, C. E., Traver, D., Mayhall, E., Shepard, J. L. and Zon, L. I. (2005). Hematopoietic stem cell fate is established by the Notch-Runx pathway. *Genes Dev.* **19**, 2331-2342.

Bussmann, J. and Schulte-Merker, S. (2011). Rapid BAC selection for tol2-mediated transgenesis in zebrafish. *Development* **138**, 4327-4332.

Chen, M. J., Yokomizo, T., Zeigler, B. M., Dzierzak, E. and Speck, N. A. (2009). Runx1 is required for the endothelial to haematopoietic cell transition but not thereafter. *Nature* **457**, 887-891.

Chen, M. J., Li, Y., De Obaldia, M. E., Yang, Q., Yzaguirre, A. D., Yamada-Inagawa, T., Vink, C. S., Bhandoola, A., Dzierzak, E. and Speck, N. A. (2011). Erythroid/myeloid progenitors and hematopoietic stem cells originate from distinct populations of endothelial cells. *Cell Stem Cell* **9**, 541-552.

Chi, N. C., Shaw, R. M., De Val, S., Kang, G., Jan, L. Y., Black, B. L. and Stainier, D. Y. R. (2008). Foxn4 directly regulates tbx2b expression and atrioventricular canal formation. *Genes Dev.* **22**, 734-739.

Ciau-Uitz, A., Monteiro, R., Kirmizitas, A. and Patient, R. (2014). Developmental hematopoiesis: ontogeny, genetic programming and conservation. *Exp. Hematol.* **42**, 669-683.

Clements, W. K. and Traver, D. (2013). Signalling pathways that control vertebrate haematopoietic stem cell specification. *Nat. Rev. Immunol.* **13**, 336-348.

Clements, W. K., Kim, A. D., Ong, K. G., Moore, J. C., Lawson, N. D. and Traver, D. (2011). A somitic Wnt16/Notch pathway specifies haematopoietic stem cells. *Nature* **474**, 220-224.

de Bruijn, M. F. T. R., Ma, X., Robin, C., Ottersbach, K., Sanchez, M.-J. and Dzierzak, E. (2002). Hematopoietic stem cells localize to the endothelial cell layer in the midgestation mouse aorta. *Immunity* **16**, 673-683.

de Pater, E., Kaimakis, P., Vink, C. S., Yokomizo, T., Yamada-Inagawa, T., van der Linden, R., Kartalaei, P. S., Camper, S. A., Speck, N. and Dzierzak, E. (2013). Gata2 is required for HSC generation and survival. *J. Exp. Med.* **210**, 2843-2850.

Detrich, H. W., III, Kieran, M. W., Chan, F. Y., Barone, L. M., Yee, K., Rundstadler, J. A., Pratt, S., Ransom, D. and Zon, L. I. (1995). Intraembryonic hematopoietic cell migration during vertebrate development. *Proc. Natl. Acad. Sci. USA* **92**, 10713-10717.

Distel, M. and Koster, R. W. (2007). In vivo time-lapse imaging of zebrafish embryonic development. *CSH Protoc.* **2007**, ppdb prot4816.

Distel, M., Wullimann, M. F. and Koster, R. W. (2009). Optimized Gal4 genetics for permanent gene expression mapping in zebrafish. *Proc. Natl. Acad. Sci. USA* **106**, 13365-13370.
Dzierzak, E. and Speck, N. A. (2008). Of lineage and legacy: the development of mammalian hematopoietic stem cells. *Nat. Immunol.* **9**, 129-136.
Force, A., Lynch, M., Pickett, F. B., Amores, A., Yan, Y. L. and Postlethwait, J. (1999). Preservation of duplicate genes by complementary, degenerative mutations. *Genetics* **151**, 1531-1545.
Gao, X., Johnson, K. D., Chang, Y.-I., Boyer, M. E., Dewey, C. N., Zhang, J. and Bresnick, E. H. (2013). Gata2 cis-element is required for hematopoietic stem cell generation in the mammalian embryo. *J. Exp. Med.* **210**, 2833-2842.
Gering, M. and Patient, R. (2005). Hedgehog signaling is required for adult blood stem cell formation in zebrafish embryos. *Dev. Cell* **8**, 389-400.
Gillis, W. Q., St John, J., Bowerman, B. and Schneider, S. Q. (2009). Whole genome duplications and expansion of the vertebrate GATA transcription factor gene family. *BMC Evol. Biol.* **9**, 207.
Guiu, J., Shimizu, R., D'Altri, T., Fraser, S. T., Hatakeyama, J., Bresnick, E. H., Kageyama, R., Dzierzak, E., Yamamoto, M., Espinosa, L. et al. (2013). Hes repressors are essential regulators of hematopoietic stem cell development downstream of Notch signaling. *J. Exp. Med.* **210**, 71-84.
Hadland, B. K., Huppert, S. S., Kanungo, J., Xue, Y., Jiang, R., Gridley, T., Conlon, R. A., Cheng, A. M., Kopan, R. and Longmore, G. D. (2004). A requirement for Notch1 distinguishes 2 phases of definitive hematopoiesis during development. *Blood* **104**, 3097-3105.
Hatta, K., Tsujii, H. and Omura, T. (2006). Cell tracking using a photoconvertible fluorescent protein. *Nat. Protoc.* **1**, 960-967.
Helker, C. S. M., Schuermann, A., Karpanen, T., Zeuschner, D., Belting, H.-G., Affolter, M., Schulte-Merker, S. and Herzog, W. (2013). The zebrafish common cardinal veins develop by a novel mechanism: lumen ensheathment. *Development* **140**, 2776-2786.
Herbomel, P., Thisse, B. and Thisse, C. (1999). Ontogeny and behaviour of early macrophages in the zebrafish embryo. *Development* **126**, 3735-3745.
Hesselson, D., Anderson, R. M., Beinat, M. and Stainier, D. Y. R. (2009). Distinct populations of quiescent and proliferative pancreatic beta-cells identified by HOTcre mediated labeling. *Proc. Natl. Acad. Sci. USA* **106**, 14896-14901.
Hong, C. C., Peterson, Q. P., Hong, J.-Y. and Peterson, R. T. (2006). Artery/vein specification is governed by opposing phosphatidylinositol-3 kinase and MAP kinase/ERK signaling. *Curr. Biol.* **16**, 1366-1372.
Itoh, M., Kim, C. H., Palardy, G., Oda, T., Jiang, Y. J., Maust, D., Yeo, S. Y., Lorick, K., Wright, G. J., Ariza-McNaughton, L. et al. (2003). Mind bomb is a ubiquitin ligase that is essential for efficient activation of Notch signaling by Delta. *Dev. Cell* **4**, 67-82.
Jaffredo, T., Gautier, R., Eichmann, A. and Dieterlen-Liévre, F. (1998). Intraaortic hemopoietic cells are derived from endothelial cells during ontogeny. *Development* **125**, 4575-4583.
Jaffredo, T., Gautier, R., Brajeul, V. and Dieterlen-Lièvre, F. (2000). Tracing the progeny of the aortic hemangioblast in the avian embryo. *Dev. Biol.* **224**, 204-214.
Johnson, K. D., Hsu, A. P., Ryu, M.-J., Wang, J., Gao, X., Boyer, M. E., Liu, Y., Lee, Y., Calvo, K. R., Keles, S. et al. (2012). Cis-element mutated in GATA2-dependent immunodeficiency governs hematopoiesis and vascular integrity. *J. Clin. Invest.* **122**, 3692-3704.
Kim, A. D., Melick, C. H., Clements, W. K., Stachura, D. L., Distel, M., Panáková, D., MacRae, C., Mork, L. A., Crump, J. G. and Traver, D. (2014). Discrete Notch signaling requirements in the specification of hematopoietic stem cells. *EMBO J.* **33**, 2363-2373.
Kissa, K. and Herbomel, P. (2010). Blood stem cells emerge from aortic endothelium by a novel type of cell transition. *Nature* **464**, 112-115.
Kissa, K., Murayama, E., Zapata, A., Cortes, A., Perret, E., Machu, C. and Herbomel, P. (2008). Live imaging of emerging hematopoietic stem cells and early thymus colonization. *Blood* **111**, 1147-1156.
Kobayashi, I., Kobayashi-Sun, J., Kim, A. D., Pouget, C., Fujita, N., Suda, T. and Traver, D. (2014). Jam1a-Jam2a interactions regulate haematopoietic stem cell fate through Notch signalling. *Nature* **512**, 319-323.
Kohli, V., Schumacher, J. A., Desai, S. P., Rehn, K. and Sumanas, S. (2013). Arterial and venous progenitors of the major axial vessels originate at distinct locations. *Dev. Cell* **25**, 196-206.
Kwan, K. M., Fujimoto, E., Grabher, C., Mangum, B. D., Hardy, M. E., Campbell, D. S., Parant, J. M., Yost, H. J., Kanki, J. P. and Chien, C.-B. (2007). The Tol2kit: a multisite gateway-based construction kit for Tol2 transposon transgenesis constructs. *Dev. Dyn.* **236**, 3088-3099.
Lam, E. Y. N., Hall, C. J., Crosier, P. S., Crosier, K. E. and Flores, M. V. (2010). Live imaging of Runx1 expression in the dorsal aorta tracks the emergence of blood progenitors from endothelial cells. *Blood* **116**, 909-914.
Lancrin, C., Sroczynska, P., Stephenson, C., Allen, T., Kouskoff, V. and Lacaud, G. (2009). The haemangioblast generates haematopoietic cells through a haemogenic endothelium stage. *Nature* **457**, 892-895.
Langenau, D. M., Traver, D., Ferrando, A. A., Kutok, J. L., Aster, J. C., Kanki, J. P., Lin, S., Prochownik, E., Trede, N. S., Zon, L. I. et al. (2003). Myc-induced T cell leukemia in transgenic zebrafish. *Science* **299**, 887-890.
Lawson, N. D. and Weinstein, B. M. (2002). In vivo imaging of embryonic vascular development using transgenic zebrafish. *Dev. Biol.* **248**, 307-318.
Li, X., Jia, S., Wang, S., Wang, Y. and Meng, A. (2009). Mta3-NuRD complex is a master regulator for initiation of primitive hematopoiesis in vertebrate embryos. *Blood* **114**, 5464-5472.
Liao, E. C., Paw, B. H., Oates, A. C., Pratt, S. J., Postlethwait, J. H. and Zon, L. I. (1998). SCL/Tal-1 transcription factor acts downstream of cloche to specify hematopoietic and vascular progenitors in zebrafish. *Genes Dev.* **12**, 621-626.
Lim, K.-C., Hosoya, T., Brandt, W., Ku, C.-J., Hosoya-Ohmura, S., Camper, S. A., Yamamoto, M. and Engel, J. D. (2012). Conditional Gata2 inactivation results in HSC loss and lymphatic mispatterning. *J. Clin. Invest.* **122**, 3705-3717.
Ma, M. and Jiang, Y.-J. (2007). Jagged2a-notch signaling mediates cell fate choice in the zebrafish pronephric duct. *PLoS Genet.* **3**, e18.
Milano, J., McKay, J., Dagenais, C., Foster-Brown, L., Pognan, F., Gadient, R., Jacobs, R. T., Zacco, A., Greenberg, B. and Ciaccio, P. J. (2004). Modulation of notch processing by gamma-secretase inhibitors causes intestinal goblet cell metaplasia and induction of genes known to specify gut secretory lineage differentiation. *Toxicol. Sci.* **82**, 341-358.
Minegishi, N., Suzuki, N., Yokomizo, T., Pan, X., Fujimoto, T., Takahashi, S., Hara, T., Miyajima, A., Nishikawa, S.-i. and Yamamoto, M. (2003). Expression and domain-specific function of GATA-2 during differentiation of the hematopoietic precursor cells in midgestation mouse embryos. *Blood* **102**, 896-905.
Mumm, J. S., Schroeter, E. H., Saxena, M. T., Griesemer, A., Tian, X., Pan, D. J., Ray, W. J. and Kopan, R. (2000). A ligand-induced extracellular cleavage regulates gamma-secretase-like proteolytic activation of Notch1. *Mol. Cell* **5**, 197-206.
Murayama, E., Kissa, K., Zapata, A., Mordelet, E., Briolat, V., Lin, H.-F., Handin, R. I. and Herbomel, P. (2006). Tracing hematopoietic precursor migration to successive hematopoietic organs during zebrafish development. *Immunity* **25**, 963-975.
Nakagawa, M., Ichikawa, M., Kumano, K., Goyama, S., Kawazu, M., Asai, T., Ogawa, S., Kurokawa, M. and Chiba, S. (2006). AML1/Runx1 rescues Notch1-null mutation-induced deficiency of para-aortic splanchnopleural hematopoiesis. *Blood* **108**, 3329-3334.
North, T., Gu, T. L., Stacy, T., Wang, Q., Howard, L., Binder, M., Marin-Padilla, M. and Speck, N. A. (1999). Cbfa2 is required for the formation of intra-aortic hematopoietic clusters. *Development* **126**, 2563-2575.
North, T. E., de Bruijn, M. F. T. R., Stacy, T., Talebian, L., Lind, E., Robin, C., Binder, M., Dzierzak, E. and Speck, N. A. (2002). Runx1 expression marks long-term repopulating hematopoietic stem cells in the midgestation mouse embryo. *Immunity* **16**, 661-672.
North, T. E., Goessling, W., Walkley, C. R., Lengerke, C., Kopani, K. R., Lord, A. M., Weber, G. J., Bowman, T. V., Jang, I.-H., Grosser, T. et al. (2007). Prostaglandin E2 regulates vertebrate haematopoietic stem cell homeostasis. *Nature* **447**, 1007-1011.
Nottingham, W. T., Jarratt, A., Burgess, M., Speck, C. L., Cheng, J.-F., Prabhakar, S., Rubin, E. M., Li, P.-S., Sloane-Stanley, J., Kong-a-San, J. et al. (2007). Runx1-mediated hematopoietic stem-cell emergence is controlled by a Gata/Ets/SCL-regulated enhancer. *Blood* **110**, 4188-4197.
Quillien, A., Moore, J. C., Shin, M., Siekmann, A. F., Smith, T., Pan, L., Moens, C. B., Parsons, M. J. and Lawson, N. D. (2014). Distinct Notch signaling outputs pattern the developing arterial system. *Development* **141**, 1544-1552.
Robert-Moreno, À., Espinosa, L., de la Pompa, J. L. and Bigas, A. (2005). RBPjkappa-dependent Notch function regulates Gata2 and is essential for the formation of intra-embryonic hematopoietic cells. *Development* **132**, 1117-1126.
Robert-Moreno, À., Guiu, J., Ruiz-Herguido, C., López, M. E., Inglés-Esteve, J., Riera, L., Tipping, A., Enver, T., Dzierzak, E., Gridley, T. et al. (2008). Impaired embryonic haematopoiesis yet normal arterial development in the absence of the Notch ligand Jagged1. *EMBO J.* **27**, 1886-1895.
Swiers, G., Rode, C., Azzoni, E. and de Bruijn, M. F. T. R. (2013). A short history of hemogenic endothelium. *Blood Cells Mol. Dis.* **51**, 206-212.
Taoudi, S. and Medvinsky, A. (2007). Functional identification of the hematopoietic stem cell niche in the ventral domain of the embryonic dorsal aorta. *Proc. Natl. Acad. Sci. USA* **104**, 9399-9403.
Tavian, M., Hallais, M. F. and Peault, B. (1999). Emergence of intraembryonic hematopoietic precursors in the pre-liver human embryo. *Development* **126**, 793-803.
Thisse, C., Thisse, B., Schilling, T. F. and Postlethwait, J. H. (1993). Structure of the zebrafish snail1 gene and its expression in wild-type, spadetail and no tail mutant embryos. *Development* **119**, 1203-1215.
Thompson, M. A., Ransom, D. G., Pratt, S. J., MacLennan, H., Kieran, M. W., Detrich, H. W., III, Vail, B., Huber, T. L., Paw, B., Brownlie, A. J. et al. (1998). The cloche and spadetail genes differentially affect hematopoiesis and vasculogenesis. *Dev. Biol.* **197**, 248-269.
Traver, D., Paw, B. H., Poss, K. D., Penberthy, W. T., Lin, S. and Zon, L. I. (2003). Transplantation and in vivo imaging of multilineage engraftment in zebrafish bloodless mutants. *Nat. Immunol.* **4**, 1238-1246.

Development (2015) 142, 1050-1061 doi:10.1242/dev.119180

Tsai, F.-Y., Keller, G., Kuo, F. C., Weiss, M., Chen, J., Rosenblatt, M., Alt, F. W. and Orkin, S. H. (1994). An early haematopoietic defect in mice lacking the transcription factor GATA-2. *Nature* **371**, 221-226.

van Es, J. H., van Gijn, M. E., Riccio, O., van den Born, M., Vooijs, M., Begthel, H., Cozijnsen, M., Robine, S., Winton, D. J., Radtke, F. et al. (2005). Notch/gamma-secretase inhibition turns proliferative cells in intestinal crypts and adenomas into goblet cells. *Nature* **435**, 959-963.

Vicente, C., Conchillo, A., García-Sánchez, M. A. and Odero, M. D. (2012). The role of the GATA2 transcription factor in normal and malignant hematopoiesis. *Crit. Rev. Oncol. Hematol.* **82**, 1-17.

Wilkinson, R. N., Pouget, C., Gering, M., Russell, A. J., Davies, S. G., Kimelman, D. and Patient, R. (2009). Hedgehog and Bmp polarize hematopoietic stem cell emergence in the zebrafish dorsal aorta. *Dev. Cell* **16**, 909-916.

Yang, Z., Gu, L., Romeo, P. H., Bories, D., Motohashi, H., Yamamoto, M. and Engel, J. D. (1994). Human GATA-3 trans-activation, DNA-binding, and nuclear localization activities are organized into distinct structural domains. *Mol. Cell. Biol.* **14**, 2201-2212.

Yokomizo, T. and Dzierzak, E. (2010). Three-dimensional cartography of hematopoietic clusters in the vasculature of whole mouse embryos. *Development* **137**, 3651-3661.

Zhang, Y., Jin, H., Li, L., Qin, F. X.-F. and Wen, Z. (2011). cMyb regulates hematopoietic stem/progenitor cell mobilization during zebrafish hematopoiesis. *Blood* **118**, 4093-4101.

Zhu, H., Traver, D., Davidson, A. J., Dibiase, A., Thisse, C., Thisse, B., Nimer, S. and Zon, L. I. (2005). Regulation of the lmo2 promoter during hematopoietic and vascular development in zebrafish. *Dev. Biol.* **281**, 256-269.

Zhu, C., Smith, T., McNulty, J., Rayla, A. L., Lakshmanan, A., Siekmann, A. F., Buffardi, M., Meng, X., Shin, J., Padmanabhan, A. et al. (2011). Evaluation and application of modularly assembled zinc-finger nucleases in zebrafish. *Development* **138**, 4555-4564.

Zovein, A. C., Hofmann, J. J., Lynch, M., French, W. J., Turlo, K. A., Yang, Y., Becker, M. S., Zanetta, L., Dejana, E., Gasson, J. C. et al. (2008). Fate tracing reveals the endothelial origin of hematopoietic stem cells. *Cell Stem Cell* **3**, 625-636.